Y10.19); IEEE Std 280-1968, *Letter Symbols for Quantities used in Electrical Science and Electrical Engineering* (ANSI Y10.5); IEEE Std 315-1971, *Graphic Symbols for Electrical and Electronics Diagrams* (ANSI Y32.2); IEEE Std 322-1971, *Rules for Use of Units of the International System of Units, and Selection of the Decimal Multiples and Submultiples*. Std 315 contains sections on antennas (which permits incorporation of antenna polarization and steerability in a set of internationally recommended symbols) and waveguides, again internationally recommended.

At present, committees in G-AP are engaged in the following standards projects. A group is working on definitions of terms and test procedures relating to antennas in physical media. IEEE Std 145-1969, is being revised and updated. Under the sponsorship of the Wave Propagation Standards Committee, there are task groups on propagation curves and prediction techniques, ionogram standardization, radio meteorology measurements, information storage and retrieval for wave propagation, methods of measuring ground conductivity, and microwave field strength measurements.

To summarize, the documents cited are of great utility to anyone engaged in testing, measurement, generation of specifications, or report writing and will also provide a practical introduction to novices in antenna and propagation technology.

Also IEEE Std. 356-1974 (AP-22 Mar 74)

First-Order Theory and Analysis of MF/HF/VHF Scatter from the Sea

DONALD E. BARRICK, MEMBER, IEEE

Abstract—Scatter from the sea near grazing from MF through VHF is analyzed in this paper. Results based on the compensation theorem show that the dependence upon the grazing angles, as well as upon frequency, range, and the effective surface impedance, can be removed for vertical polarization as the familiar "Norton attenuation factors." Time variation of the surface is included, and results are derived for both the average received power and its spectral density. The first-order dispersion relationship for gravity waves is used to show that the received spectrum from a patch of sea consists of two discrete Doppler shifts above and below the carrier, predictable from simple Bragg diffraction considerations. Using the Phillips wind-wave model as an upper limit for wave heights, estimates for σ^0 (radar cross section per unit area) of -17 dB are obtained near grazing. Both the magnitude of σ_{vv}^0 predicted from theory and the nature of the received spectrum are compared with measurements, and the agreement supports the theory on both counts. Finally, the use of MF/HF radars for measuring sea state is suggested and discussed.

I. INTRODUCTION

SEA ECHO at frequencies below VHF has been observed by radars since World War II. Crombie [1] in 1955 appears to have been the first to correctly deduce the physical mechanism producing sea scatter. Based upon HF experimental observations of the backscatter Doppler spectrum, he noted that the discrete frequency shifts of the sea echo above and below the carrier corresponded uniquely with the shifts that would be produced by ocean waves moving toward and away from the radar having lengths precisely one half the radio wavelength. Hence the mechanism was seen to be "Bragg scatter," the same phenomenon responsible for scatter of X-rays in crystals and light rays from diffraction gratings and holograms.

Quantitative theoretical analyses of the scatter problem lagged these experimental deductions by several years. Peake [2] appears to have been the first to reduce the classic boundary perturbation theory of Rice [3] to σ^0, the normalized scattering cross section per unit area for a slightly rough surface. Barrick and Peake [4] noted that this result, when interpreted, shows that scatter is produced via the Bragg mechanism, in agreement with Crombie's deductions. No attempt was made at that time to apply the theory to the sea, which was a unique wave height spectrum[1] and spatial–temporal wavenumber dispersion relationship. Thus in this paper we include the

[1] Guinard and Daley [5] have employed the "slightly rough" model derived from perturbation analysis, along with a Phillips wave height spectrum, to explain the diffuse component in microwave scatter from the sea. Since the ocean surface is "composite" at those frequencies and thus more difficult to analyze, a rigorous mathematical justification of this result is not possible. Their empirical comparisons, however, leave little doubt that this simple model is reasonably valid even at microwave frequencies, so long as one is not too close to the specular direction or to grazing. Those results along with the spectral measurements of Wright [6] and Bass *et al.* [7], show that the Bragg effect also produces scatter above VHF; this paper concentrates on analysis and comparisons below VHF, where more rigorous mathematical justification and interpretation is possible.

temporal motion of the sea surface and derive a result for the average received signal spectrum, as well as σ^0. Furthermore, we analyze in detail the region near-grazing incidence for vertical polarization and show how the behavior of backscatter varies with grazing angle for frequencies below 100 MHz. Using the Phillips ocean wave height spectrum in the model, the predicted results are compared with HF measurements, both with regard to the signal spectrum and σ^0. Limitations of the first-order theory are pointed out. Finally, the exciting possibility of using MF/HF radars to measure sea state is discussed in light of the theory.

Many previous theoretical analyses of rough surface scatter were based upon the Kirchhoff (or physical optics) integral approach (see Beckmann and Spizzichino [8], or Ruck et al. [9]). While the physical optics approach leads to Bragg scatter also (e.g., Parkins [10] derives the received spectrum of acoustic signals scattered from the sea surface with this approach), polarization dependence and near-grazing behavior is lost with that technique. Measurements, however, show that σ_{vv}^0 for near-grazing backscatter is considerably greater than σ_{hh}^0, which is in agreement with results derived from the perturbation theory. In addition, the radius of curvature of the surface need not be much greater than wavelength in the perturbation theory, as it must with physical optics.

The Rice boundary perturbation approach employs the following restrictions: 1) the height of the surface must be small in terms of radio wavelength, 2) surface slopes must be small, and 3) the impedance of the surface medium must be small in terms of the free-space wave impedance. These conditions are all satisfied by the sea below mid-VHF; the upper limit on frequency in terms of sea state will be examined in Section VI.

II. RERADIATION TO A POINT ABOVE AN IMPERFECT SURFACE

In this section we analyze the problem of scatter from the imperfectly conducting rough sea in a manner different from conventional treatments [2], [4]. We are not concerned in this section with the interaction and scatter mechanism; that will be treated in the next section. Rather, we consider separately an elemental patch of sea dS' as shown in Fig. 1. Energy is incident upon this patch from an arbitrary angle and is reradiated (or scattered) from the patch due to the roughness. The size of the patch is to be small with respect to the distance R_0 to the scattering point, but large with respect to λ the radio wavelength. Thus if the patch were reradiating in the absence of the surrounding imperfect surface, the field at the observation point would diverge as $1/R_0$. The same would be true if the surrounding surface were a perfectly conducting smooth plane, with an additional factor of 2 to account for the image.

In including the effects of imperfect conductivity and roughness of the sea surrounding dS', we assume 1) that the mean surface near dS' is planar, and 2) that an effective impedance $\bar{\Delta}$ can be assigned to the surface to account
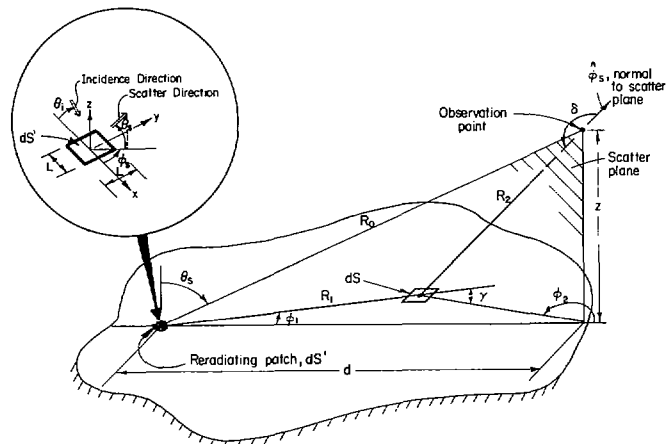

Fig. 1. Geometry for reradiation (scatter) from patch dS' used with compensation theorem.

for both its finite conductivity and roughness. The concept of normalized surface impedance was popularized by Wait [11]; this quantity is normalized with respect to the wave impedance of free space $(\mu_0/\epsilon_0)^{1/2}$ and is a function of the reradiation angle θ_s, as well as the surface parameters. We intend to employ the "compensation theorem" attributed to Monteath [12] and applied by King [13] to the problem of radiation from a dipole above an imperfect half space. In fact, the analysis here parallels that of King; the scattering behavior of the reradiating patch can in reality be modeled by a collection dipoles.

We are interested here only in the vertically polarized scattered far-field component; this can be easiest obtained by employing H_φ the azimuthal magnetic field. King shows in [13, eqs. (6) and (7)] that an integral equation in H_φ can be obtained from the compensation theorem as follows:

$$H_\varphi^{s'} = H_\varphi^s + \frac{ik_0}{2\pi} \int_s \bar{\Delta} H_\varphi^{s'} \left(\frac{\exp{(ik_0 R_2)}}{R_2} \right) \sin \delta \cos \gamma \, dS$$

(1)

where the indicated angles are shown in Fig. 1. Here H_φ^s is called the "unperturbed" H field at the observation point, and $H_\varphi^{s'}$ is the "perturbed" H field. The integration takes place at dS, a distance R_1 from the reradiating point; at this point, the effective surface impedance is described by $\bar{\Delta}$. The time dependence $\exp{(-i\omega t)}$ is assumed here.

The perturbed field here denotes the unknown quantity we are seeking, whose nature depends upon the surface over which it propagates. The unperturbed solution H_φ^s is presumed known and can be selected so as to simplify solution of the integral equation in $H_\varphi^{s'}$. Following King, we select for H_φ^s the far-zone field reradiated from the surface patch dS' *when the remainder of the surface is smooth and perfectly conducting* (i.e., $\bar{\Delta} = 0$); for now we write it as

$$H_\varphi^s = \frac{ik_0 L^2 \exp{(ik_0 R_0)}}{2\pi R_0} G_\varphi^c$$

(2)

where G_φ is a quantity to be determined in the next section. The preceding equation places in evidence the $1/R_0$ dependence of the field above the perfectly conducting smooth plane.

Following King [13], we define the perturbed field as equal to the unperturbed field times an unknown slowly varying attenuation function, i.e.,

$$H_\varphi{}^{s'} = H_\varphi{}^s F(d,z,\bar\Delta).$$

Then (1) can be rewritten as an integral equation in F, obtaining

$$F(d,z,\bar\Delta) = 1 + \frac{ik_0 R_0 \exp{(-ik_0 R_0)}}{2\pi G_\varphi(0)}$$

$$\cdot \int_s \bar\Delta G_\varphi(\varphi_1) \left(\frac{\exp{[ik_0(R_1 + R_2)]}}{R_1 R_2} \right)$$

$$\cdot F(R_1,0,\bar\Delta) \cdot \sin\delta \cos\gamma \, dS \qquad (3)$$

where $G_\varphi(0)$ is G_φ evaluated at the observation point (θ_s,φ_s), while $G_\varphi(\varphi_1)$ is G_φ evaluated at the integration point $(\pi/2,\varphi_s + \varphi_1)$.

We now note for highly conducting surface where $|\bar\Delta| \ll 1$, that F is close to unity and the preceding integral is nearly zero. It is only when the observation point is near the surface (i.e., $\pi/2 - \theta_s \simeq z/d \ll 1$) that the incident and reflected waves cancel, and only the surface wave remains. Therefore, the integral term in (3) is important for θ_s very near $\pi/2$, typically within $1°$ of grazing for seawater at HF. In this region near the Brewster angle $\bar\Delta$ and $G_\varphi(\varphi_1)$ appearing in the integrand are nearly constant over the important region near the baseline where $\varphi_1 \simeq 0$ and $\theta_s \simeq \pi/2$. By the same reasoning, $\sin\delta \simeq 1$, and $\cos\gamma \simeq 1$, so that the integral equation simplifies to

$$F(d,z,\bar\Delta) \simeq 1 + \frac{ik_0 R_0 \exp{(-ik_0 R_0)}}{2\pi} \bar\Delta$$

$$\cdot \int F(R_1,0,\bar\Delta) \left(\frac{\exp{[ik_0(R_1 + R_2)]}}{R_1 R_2} \right) dS. \qquad (4)$$

The solution to (4) is straightforward and is performed by King [13], [14]; the details will not be repeated here. He employs an elliptic coordinate system as a basis for the surface integral; he performs a stationary phase integration in the φ_1 direction, and the result reduces to an inhomogeneous Volterra integral equation of the second kind. This is then solved by Laplace transform techniques, and $F(d,z,\bar\Delta)$ is shown to be identically the "Norton attenuation factor" of ground wave theory. The only approximation (other than the far-zone assumption) on which solution of (1) is based is that [13] $|\bar\Delta_r| \ll 1$, where $\bar\Delta_r$ is the real part of $\bar\Delta$.

Thus in this section we have shown that a patch of sea reradiating (or scattering) vertically polarized electromagnetic energy over an imperfect surface does so in a manner identical to a vertical dipole located on the same plane. Within the restrictions of the analysis, therefore,

one merely solves the problem of scatter of vertically polarized waves by a perfectly conducting sea and multiplies by F, the Norton attenuation factor, to account for propagation near grazing from the patch dS' to the observation point. A similar factor must be used to account for propagation from the transmitter to the scattering patch if this path is near grazing also.

III. Scatter from a Moving Slightly Rough Surface

In the preceding section it was shown possible to express the scattered field from a patch of sea in terms of the Norton attenuation factor F times the unperturbed scattered field. This unperturbed field is to be determined in this section. It is the field scattered from the patch with the sea treated as a perfect conducting surface; the effect of finite conductivity is already accounted for in F. Below VHF the sea is "slightly rough," satisfying the restrictions mentioned in the Introduction for applicability of the boundary perturbation approach.

The first-order solution for scatter from a *stationary* random perfectly conducting surface using this approach is well-known [2], [4], [9]. We intend to extend this analysis to the case of a *moving* perfectly conducting surface, so that the temporal spectrum of the scattered signal can be obtained. We concentrate on only the vertical polarization states, since near-grazing propagation over the highly conducting sea at these frequencies is much larger for vertical than for horizontal. However, we will provide answers for the other linear polarization combinations also.

The inclusion of time as an independent variable in the description of the random surface height ζ is readily accomplished by a Fourier series expansion over time as well as space:

$$\zeta(x,y,t) = \sum_{m,n,l=-\infty}^{\infty} P(m,n,l) \exp{\{ia(mx + ny) - iwlt\}} \qquad (5)$$

where $a = 2\pi/L$ and $w = 2\pi/T$; L and T being defined as the spatial (both x and y) and temporal period of the surface. $P(m,n,l)$ is the coefficient of the m,n,lth Fourier component, with P being zero for $m = n = 0$ (i.e., the coordinate system is chosen so that the x–y plane is the mean surface). The minus sign before the time argument places in evidence the expected traveling nature of ocean waves, i.e., a wave with $+am$ and $+wl$ wavenumbers in the $+x$ direction.

Following Rice [3] we define an average spatial–temporal spectrum $W(p,q,\omega)$ of the surface height in terms of the Fourier coefficients as

$$W(p,q,\omega) = \frac{1}{\pi^3} \iiint_{-\infty}^{\infty} \langle \zeta(x_1,y_1,t_1) \zeta(x_2,y_2,t_2) \rangle$$

$$\cdot \exp{(ip\tau_x + iq\tau_y - i\omega\tau)} \, d\tau_x \, d\tau_y \, d\tau$$

$$= \frac{L^2 T}{\pi^3} \langle P(m,n,l) P(-m,-n,-l) \rangle \qquad (6)$$

where $\langle P(m_1,n_1,l_1)P(m_2,n_2,l_2)\rangle$ is zero when $m_2 \neq -m_1$, $n_2 \neq -n_1$, and $l_2 \neq -l_1$ because the Fourier coefficients are uncorrelated. Also, $p = am$, $q = an$, $\omega = wl$, $\tau_x = x_2 - x_1$, $\tau_y = y_2 - y_1$, and $\tau = t_2 - t_1$ in (6). The angular braces $\langle \cdot \rangle$ denote a statistical ensemble average. Also, $\langle P(m,n,l)\rangle = 0$, for all m,n,l.

The total fields above the surface (see Fig. 1 inset for scatter geometry) are represented by plane-wave (eigenfunction) expansions of the same form as (5)

$$E_x = \frac{b(\nu,0)}{k_0}\left[E(\nu,0,0;z) - E(-\nu,0,0;z)\right]$$

$$+ \sum_{m,n,l=-\infty}^{\infty} A_{mnl}E(m+\nu,n,l;z) \quad (7a)$$

$$E_y = \sum_{m,n,l=-\infty}^{\infty} B_{mnl}E(m+\nu,n,l;z) \quad (7b)$$

$$E_z = \frac{a\nu}{k_0}\left[E(\nu,0,0;z) + E(-\nu,0,0;z)\right]$$

$$+ \sum_{m,n,l=-\infty}^{\infty} C_{mnl}E(m+\nu,n,l;z) \quad (7c)$$

where

$$E(m+\nu,n,l,z) = 2E_0 \exp\{ia(m+\nu)x + iany$$
$$+ ib(m+\nu,n)z - i(wl+\omega_0)t\}$$

and

$$b(m+\nu,n) = [k_0^2 - a^2(m+\nu)^2 - a^2n^2]^{1/2}.$$

Here $\nu = k_0 \sin\theta_i/a$, and the two terms in square brackets in (7a) and (7c) are the incident and reflected plane waves from the perfectly conducting surface in the absence of roughness. The incident electric field strength E_0 is normalized such that the *total* vertical component at the surface for incident propagation near grazing is $2E_0$.

The solution for the unknown scattered field coefficients A_{mnl}, etc., is straightforward. In fact, these coefficients are identical to the first-order coefficients A_{mn}, etc., derived by Rice in [3, eq. (4.2)] with three notation differences: 1) his $m - \nu$ is our m; 2) his i is our $-i$ because of a difference in sign in our time conventions; 3) our A_{mnl}, etc., are directly proportional to $P(m,n,l)$, whereas his are proportional to $P(m,n)$; the factors of proportionality however, are the same.

It is now necessary to relate the modal fields scattered by an infinite periodic random surface to the field scattered by a finite patch of area dS' of such a surface. This is again straightforward and can follow the geometrical arguments of Peake [2] and Barrick and Peake [15] or a Kirchhoff-type transformation of Barrick [16]; the reader is referred to these treatments. Basically, the result shows that the field strength falls off as $1/R_0$, as it should, and relates the modal field wavenumbers $a(m - \nu)$, an, and $b(m + \nu,n)$ to the scattered field direction cosines $\sin\theta_s \cos\varphi_s$, $\sin\theta_s \sin\varphi_s$, and $\cos\theta_s$.

The average scattered power correlation function at two different times is then computed, i.e.,

$$\langle E_v^s(R_0,t_1)E_v^{s*}(R_0,t_2)\rangle \equiv R^s(\tau)$$

where $\tau = t_2 - t_1$. The Fourier transform of this then gives the average scattered signal spectrum in terms of $W(p,q,\omega)$ as defined in (6). Details can be found in Barrick [16].

IV. AVERAGE SCATTER CROSS SECTIONS AND THE RADAR RANGE EQUATION

The average scattered signal power density spectrum can now be converted to $\sigma_{vv}(\omega)$ the average scatter cross section per unit area per rad/s bandwidth; its integral is the familiar σ_{vv}^0, i.e., $\sigma^0 = 1/2\int_{-\infty}^{\infty}\sigma(\omega)\,d\omega$, which is

$$\left.\begin{array}{c}\sigma_{vv}(\omega)\\ \\ \sigma_{vv}^0\end{array}\right\} = 4\pi k_0(\sin\theta_i \sin\theta_s - \cos\varphi_s)^2$$

$$\times \left\{\begin{array}{l} W[k_0(\sin\theta_s \cos\varphi_s - \sin\theta_i), \\ \qquad k_0\sin\theta_s\sin\varphi_s, \quad \omega - \omega_0] \quad (8a)\\ \\ W[k_0(\sin\theta_s \cos\varphi_s - \sin\theta_i), \\ \qquad\qquad k_0\sin\theta_s\sin\varphi_s] \quad (8b)\end{array}\right.$$

where the spatial spectrum $W[p,q]$ is obtained from $W[p,q,\omega]$ by integration over ω and division by 2. Both spectra have the wavenumbers p,q, replaced by $k_0(\sin\theta_s \cos\varphi_s - \sin\theta_i), k_0\sin\theta_s\sin\varphi_s$. The latter are precisely the wavenumbers required of a diffraction grating which is to scatter a wave incident from θ_i into a direction θ_s,φ_s. Hence the theory shows that the ocean surface produces scatter by the simple Bragg mechanism, which confirms the experimental deductions of Crombie [1].

Although they are not of interest in this paper, the other three cross section spectra for a perfectly conducting surface $\sigma_{vh}(\omega),\sigma_{hv}(\omega)$, and $\sigma_{hh}(\omega)$ are obtained by replacing the factor $(\sin\theta_i \sin\theta_s - \cos\varphi_s)^2$ in (8a) by $(\cos\theta_i \sin\varphi_s)^2$, $(\cos\theta_s \sin\varphi_s)^2$, and $(\cos\theta_i \cos\theta_s \cos\varphi_s)^2$, respectively. The same substitution is made in (8b) also. Thus the dependence upon the nature of the roughness is the same for any polarization state; it is contained in the surface height spatial-temporal spectrum.

The average power energy density and power received in a bistatic radar system, $dP_R(\omega)$ and dP_R, from a patch of sea dS' located at distances R_T and R_R from the transmitter and receiver can now be written

$$\left.\begin{array}{c}dP_R(\omega)\\ \\ dP_R\end{array}\right\} = \frac{P_T G_T^0 G_R^0 \lambda^2}{(4\pi)^3 R_T^2 R_R^2}F_T^2 F_R^2 dS'$$

$$\times \left\{\begin{array}{ll}\sigma_{vv}(\omega), & \text{W/rad/s} \quad (9a)\\ \\ \sigma_{vv}^0, & \text{W} \quad (9b)\end{array}\right.$$

where P_T is the average transmitted power and G_T^0 and G_R^0 are the transmitting and receiving antenna gains (defined with respect to free space) in the direction of the patch. The quantities F_T^2 and F_R^2 are the Norton attenuation factors. The use of F_R^2 was justified in Section II to account for the imperfect nature of the surface medium

in the analysis of propagation from the patch dS'. It of course has significance here only for scattered vertical polarization, and is a function of range R_R to the receiver. A similar and even more obvious use of the compensation theorem shows that F_T^2 accounts for propagation of a vertically polarized field from the transmitter to the patch.

The Norton attenuation factor (e.g., F_R) appearing in the preceding equation is a function of the effective surface impedance $\bar{\Delta}$, of range R_R, and finally of the height of the receiver above the surface. Hence it contains the "dependence upon grazing angle" produced by the finite conductivity of the surface medium. It is normalized, and approaches unity as $R_R \to 0$ and for sufficiently small $\bar{\Delta}$. In this limit, one has in (9) the conventional radar range equation above a perfectly conducting flat plane. While F_R was defined for a "flat" surface, the definition can be extended to a "spherical" surface, in which case F_R is found, for example, from a residue series [11] when the observation point is distant and below the horizon.

One must be cautious in the definition of σ^0. Had one defined σ^0 in terms of $2E_0$ the total near-grazing field, rather than the *incident* field, the factor of 4 appearing in (8) would be missing; this alternate definition [8] might be considered more appropriate for ground-wave propagation. On the other hand, others include factors of 4 in the antenna gains by measuring their efficiencies *in the presence of the highly conducting ground* rather than in terms of their equivalent gains in free space. The reasoning behind the definition appearing in (8) and (9) is that propagation effects (i.e., the factors of 4, as well as F_R and F_T) due to the medium are clearly separated from the parameters describing the transmitter (G_R^0), the scatterer (σ^0), and the receiver (G_R^0). Because of widespread differences, however, reported values of σ^0 can vary by as much as 16 merely due to the definition employed.

V. First-Order Ocean Waves and the Phillips Model

It has been shown that Bragg scatter from the larger gravity waves (longer than 1 m) produces the return at HF. Such gravity waves have a unique first-order dispersion relationship. The latter makes it possible to relate the spatial–temporal height spectrum $W(p,q,\omega)$ to the simpler spatial spectrum $W(p,q)$. Stated simply, deep-water gravity waves of length L travel at a given phase velocity $v_w = (gL/2\pi)^{1/2}$, where $g \approx 9.81$ m/s^2 is the acceleration of gravity. This first-order velocity expression provides the dispersion relationship between the temporal and spatial wavenumbers of gravity waves:

$$\omega_g = +[g(p^2 + q^2)^{1/2}]^{1/2} = +[g(a^2m^2 + a^2n^2)^{1/2}]^{1/2}. \quad (10)$$

Thus the more general (5) for the height of a moving random surface reduces to the following in the case of ocean waves moving into the $+x$ half space:

$$\zeta(x,y,t) = \sum_{m,n=-\infty}^{\infty} P_+(m,n)$$
$$\cdot \exp[iamx + iany - i\,\mathrm{sgn}\,(m)\omega_g t] \quad (11)$$

where sgn (m) is ± 1, for $m\pm$. A similar expression holds for ocean waves moving into the $-x$ half space, with P_+ replaced by P_- and a plus sign in front of the last term of the exponential. Thus two sets of coefficients P_+ and P_- are called for, depending upon the strengths of the various Fourier components moving in the $+x/-x$ directions. Using (6) we can determine $W(p,q,\omega)$ from (11) by multiplying $\zeta(x_1,y_1,t_1)$ by $\zeta(x_2,y_2,t_2)$, averaging, and taking the Fourier transform. We then obtain

$$W(p,q,\omega) = 2W_+(p,q)\delta(\omega + \mathrm{sgn}\,(p)\omega_g)$$
$$+ 2W_-(p,q)\delta(\omega - \mathrm{sgn}\,(p)\omega_g) \quad (12)$$

where $W_{\pm}(p,q) = \langle|\,P_{\pm}(m,n)\,|^2\rangle L^2/\pi^2$ and $\delta(x)$ is the impulse function of argument x.

Equation (12) simply means that for a given set of spatial wavenumbers p,q, only one temporal wavenumber ω_g is possible, as given by (10). When (12) is substituted into (8a), we see that the signal scattered from an infinitesimal patch of ocean dS' occurs at two unique Doppler shifts from the carrier, as represented by the impulse functions. The shifts are determined from substituting the arguments appearing in place of p,q in (8a) into (10) to obtain

$$\omega_g = +(gk_0)^{1/2}[\sin^2\theta_s - 2\sin\theta_s \sin\theta_i \cos\varphi_s + \sin^2\theta_i]^{1/4}. \quad (13)$$

This Doppler shift corresponds to a velocity for those ocean waves having the proper length for Bragg scatter. The shift is zero for forward scatter where $\theta_s = \theta_i$ and $\varphi_s = 0$. It is largest for backscatter at grazing, where $\theta_s = \theta_i = \pi/2$, $\varphi_s = \pi$; here $\omega_g = +(2k_0g)^{1/2}$, and the length of the ocean waves responsible for scatter is the shortest, i.e., $L = \lambda/2$.

In order to obtain a rough feeling for the magnitude of ocean wave scatter, we employ a semiempirical model for $W(p,q)$ proposed by Phillips [17] and Munk and Nierenberg [18]. This model relates the roughness height to the wind blowing across the water. The model neglects swell, that is, waves due to storms in other areas which propagate to the region of interest. In addition, the model assumes that the winds have been blowing for a sufficient time that the ocean waves are fully developed. This time period may exceed 20 h for the longer ocean waves. Based on neglect of possible swell, the model has the form

$$W(p,q) = \frac{2 \times 10^{-2}}{\pi(p^2 + q^2)^2}\ \mathrm{m}^4 \quad (14)$$

where the spectrum is assumed to be identically zero when $(p^2 + q^2)^{1/2} < g/U^2$ (U = wind velocity in m/s) and also in the half space of the p–q plane from which the wind is blowing. The dimensionless constant 2×10^{-2} has been estimated as high as 4×10^{-2} by some [17]. The preceding spectrum is semiisotropic rather than highly directional; wave slope measurements by Cox and Munk [19] lead them to believe that a highly directional spectrum is difficult to justify [18].
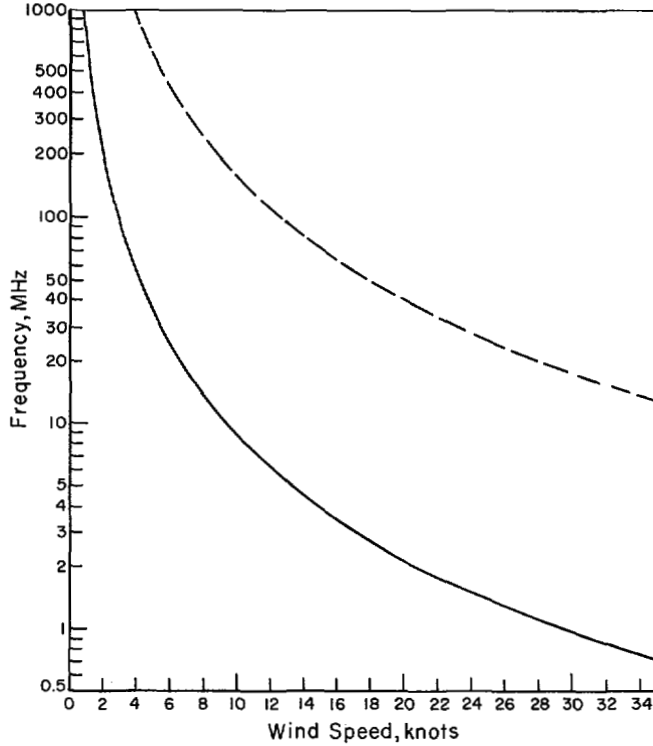
Fig. 2. Solid curve gives frequency necessary to observe lower end (cutoff) of gravity wave spectrum versus frequency for near-grazing backscatter. Dashed curve gives frequency limit where slightly rough surface model fails for given wind speed.

We now introduce the Phillips spectrum into (8), but restrict our attention to the case where both the transmitter and receiver are near the surface, i.e., θ_s, $\theta_i \rightarrow \pi/2$. We then obtain

$$\sigma(\omega) = 4 \times 10^{-2} \left[f_{+}\delta \left(\omega - \omega_0 + \left(2gk_0 \sin \left(\frac{\varphi_s}{2} \right) \right)^{1/2} \right) \right.$$

$$\left. + f_{-}\delta \left(\omega - \omega_0 - \left(2gk_0 \sin \left(\frac{\varphi_s}{2} \right) \right)^{1/2} \right) \right] \quad (15)$$

$$\sigma^0 = 0.02 = -17 \text{ dB} \quad (16)$$

where f_{+} and f_{-} represent the fraction of spectral energy in the forward-moving $(+x)$ and backward-moving $(-x)$ ocean waves, with $f_{+} + f_{-} = 1$.

Section VII compares the preceding prediction for σ_{vv}^0 of -17 dB with measurements. It should be noted that the Phillips model predicts no dependence of σ_{vv}^0 on frequency, assuming that the sea is fully developed with $U^2 > g/(p^2 + q^2)^{1/2}$; for wind speeds below this limit σ_{vv}^0 is predicted to be zero. Obviously this abrupt cutoff is not physically realized in nature due to swell and incomplete wind development. We plot in Fig. 2 the idealized lower wind cutoff of near-grazing backscatter with frequency, nonetheless, to obtain a feel for the frequencies necessary to observe the lower end of the gravity wave spectrum. Also shown is the frequency at which the height requirement for the slightly rough surface analysis fails (i.e.,

where $k_0^2 \langle \zeta^2 \rangle = 0.2$) versus wind speed; for the Phillips spectrum, $\langle \zeta^2 \rangle = (10^{-2}/4) \times U^4/g^2$. The slope requirement is always satisfied, even when the sea is fully developed, or saturated; higher winds cause breaking and dissipation of wave energy at a saturated wavenumber, hence maintaining the Phillips value as an upper limit.

VI. NEAR-GRAZING BEHAVIOR

Equation (9b) for the received power (the radar range equation) exhibits a dependence with grazing angle as contained explicitly in the factors $F_T^2 F_R^2 \sigma_{vv}^0$. The factor σ_{vv}^0 alone, however, is nearly a constant near grazing $(\theta_s, \theta_i \simeq \pi/2)$, as can be seen from (8b) and (16). Hence any decrease near grazing due to the imperfect nature of the surface is contained in the Norton attenuation factors F_T^2, F_R^2.

One might have alternately defined the scatter cross section per unit area directly from the radar range equation as $\sigma_{vv}^{0\prime} = F_T^2 F_R^2 \sigma_{vv}^0$ (give or take a factor of 16, depending upon how the antenna gains are normalized). This $\sigma_{vv}^{0\prime}$, which might be a more logical definition for an experimentalist reducing his data, will obviously depend upon the surface impedance and grazing angle. However, this dependence will not be simple; furthermore, $\sigma_{vv}^{0\prime}$ will also depend upon the ranges R_T and R_R to the scattering patch.

In order to study the dependence of $\sigma_{vv}^{0\prime}$ upon grazing angle for the sea, we specialize to backscatter, where $\varphi_s = \pi$ and $F_R = F_T$. Then $\sigma_{vv}^{0\prime} = F_R^4 \sigma_{vv}^0$. We consider also a spherical earth; therefore, F_R does not have a simple closed form, especially for short ranges and near the penumbra. To evaluate F_R, we employ a computer program developed at ITS [20]. The value $\bar{\Delta}$ employed to describe the imperfect nature of the sea surface contains both Δ, the wave impedance of ocean water ($\epsilon = 81\epsilon_0$, $\sigma = 4$ mho/m), as well as the increase due to roughness (see Barrick [21] for a treatment of the latter effect).

Fig. 3 shows the predicted dependence of $\sigma_{vv}^{0\prime}$ on grazing angle over the sea at 10 and 100 MHz using the Phillips spectrum (14) in (8b). The cutoff criterion for this model implies that σ^0 should follow these curves up to a grazing angle α given by $\cos^{-1}[\lambda g/4\pi U^2]$; the backscatter should drop to zero for directions closer to normal than this "cutoff" angle. The angular region near grazing is shown enhanced by a logarithmic abscissa scale; in addition, we display the predicted dependence beyond the horizon, i.e., when dS' is in the earth's shadow of the radar. Also shown are σ_{hh}^0 the horizontal cross section.

The figures show that near grazing, sea scatter for vertical polarization is strongly dependent upon frequency. At MF and HF it is possible to obtain sea clutter echo from below the horizon for moderate ranges. At VHF, however, the Norton attenuation factor decreases so rapidly near grazing that one could expect below-the-horizon clutter only from very short ranges (less than 10 km).
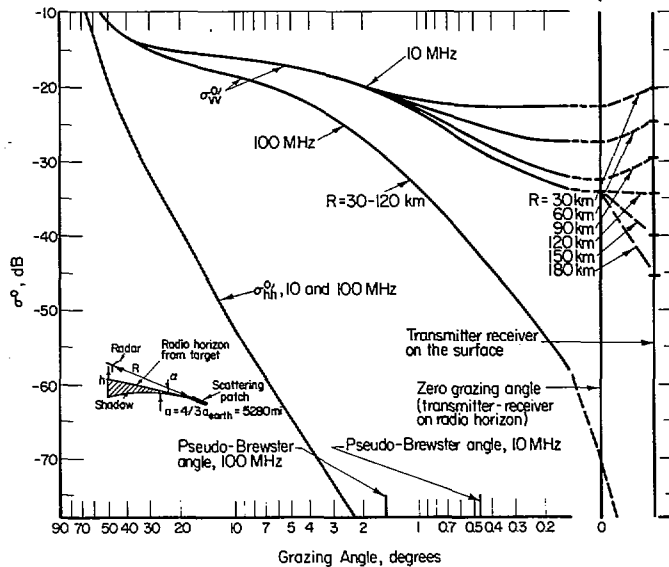
Fig. 3.   Dependence of received backscatter power on grazing angle (including Norton attenuation factors in $\sigma_{vv}^{0\prime}$) for Phillips wind-wave spectrum.

Fig. 4.   Measured ocean backscatter signal spectrum at 2.9 MHz (after Crombie, et al. [21]).

VII. COMPARISON WITH MEASUREMENTS

While many persons have observed near-grazing sea clutter at HF and VHF, few have taken the effort to calibrate their radar parameters so as to permit determination of σ^0. One recent experiment at 10.087 MHz was performed by Headrick of the Naval Research Laboratory (NRL) [22], in which he obtained estimates of σ_{vv}^0. In this experiment, two vertical monopoles were located near Annapolis, Md., on the upper Chesapeake Bay in a monostatic radar configuration. Spectral processing permitted separation of water-wave scatter from stationary ground clutter echoes. A coded signal format permitted a 20-nmi range resolution cell. The Norton attenuation factor F_R was calculated for four different range cells on the bay using the pertinent water conductivity (i.e., $\sigma \simeq 2$ mho/m).

Data were recorded and processed on February 4, 1969, a day on which a moderate wind was blowing from the north. Waves receding from the radar were observed to be stronger due to the wind, and water waves of the Bragg scatter length (15 m in this case) were estimated to be fully developed. The averaged received power was processed at four ranges down the bay: 45, 55, 67, and 75 nmi. Propagation to all of these points was via ground wave *since they were all below the radio horizon*. The area within each resolution cell dS' was estimated from maps of the bay. When cast in the form of (9b) with the attenuation factors removed, σ_{vv}^0 was measured to be -17 dB at all four ranges.[2]

The fact that the water surface in this case was fairly rough means that the backscatter might have been expected to approach the Phillips wind-wave estimate from (16) as an upper limit. The agreement between measured

Fig. 5.   Measured ocean backscatter signal spectrum at 8.37 MHz (after Crombie, et al. [21]).

and predicted values of σ_{vv}^0 not only lends credence to the theory, but confirms the oceanographic estimate of the "Phillips saturation constant" of 2×10^{-2} used in (14).

As further evidence of the validity of the first-order theory for ocean-wave scatter, we cite recent HF measurements by Crombie et al. [23] from Barbados Island in the West Indies. Again the antennas were located near the water so that propagation to ranges beyond the horizon was via ground wave. In this case, absolute estimates of σ^0 were not reported, but very accurate digital processing permitted detailed resolution of the received signal spectrum. Backscatter was received with broad-band vertical monopole antennas from the half space toward the east.

Shown in Figs. 4 and 5 are the received power spectra measured simultaneously on August 15, 1969 at 2.9 and

---

[2] Headrick reports the actual antenna gains rather than the free-space gains. Hence his reported values of -29 dB correspond to σ_{vv}^0 of -17 dB by our definition.
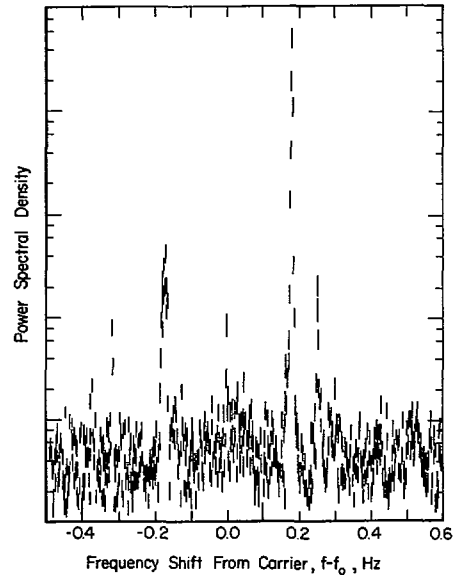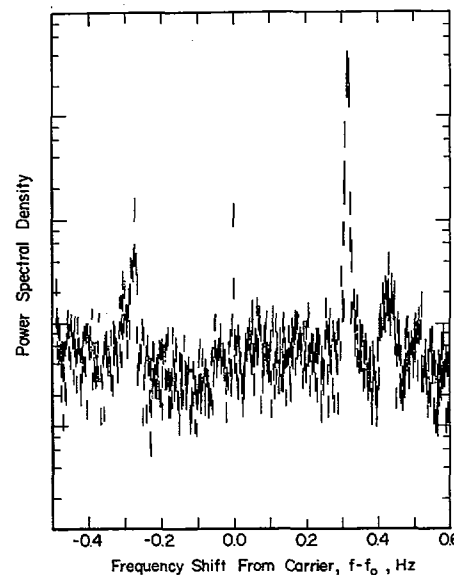
8.37 MHz from the range cell at 45 km. The processor permitted 0.002-Hz resolution; coherent processing at an offset of 0.5 Hz (removed in the figures) permits both negative and positive shifts about the carrier to be observed. The first-order peaks (corresponding to our impulse functions of (12)) occur at ±0.174 Hz from the carrier at 2.90 MHz and at ±0.296 Hz at 8.37 MHz. The relative strength of the positive spike over the negative spike at both frequencies agrees with the dominant wind direction in this area; trade winds from the east should excite west-moving water waves, producing a positive Doppler shift.

Lesser spikes in the records at 0.0 Hz, +0.25 Hz (in Fig. 4) and +0.42 Hz (in Fig. 5) are attributed by Crombie as due to nonlinearities in both the water-wave equations and scattering process. Section VI estimated the spatial–temporal spectrum based upon a linear hydrodynamic theory of water waves and the first-order terms in the perturbation analysis.

VIII. DISCUSSION AND CONCLUSIONS

This paper set forth a simple closed-form result for both σ^0 and the average scattered signal spectrum from a moving sea surface, based upon a straightforward first-order hydrodynamic and electromagnetic analysis. The discrete Bragg-produced Doppler shifts [1], [23], observed experimentally manifest themselves in the impulse spectral functions contained in our result. Our quantitative estimates for σ_{tv}^0 of -17 dB are shown to agree with measurements also. Limits on the mathematical validity of the boundary perturbation approach are derived in terms of frequency and sea state.

We showed that the effect of incidence or scatter of vertically polarized waves near grazing could be separated from σ^0 as the Norton attenuation factors. These factors are not only functions of the effective surface impedance, frequency, and the propagation angles, but also of range. These factors can also conveniently account for sea scatter *below the horizon*, where concepts of incidence and scattering angles no longer have meaning. It appears more sound to separate these propagation factors from the radar scattering cross section, as we are suggesting in this paper, for two reasons: 1) their interpretation is clear and their origin is unrelated to the mechanism producing scatter, and 2) σ_{vt}^0 then approaches a more universal constant value near grazing, independent of range to the scattering patch.

Several have suggested earlier (Crombie [1], Ward [24], etc.) that MF/HF radars should prove to be extremely useful tools for remote sensing of sea state. With the analysis presented in this paper, we have provided a quantitative link between the radar observables and the ocean-wave height spectrum which will be essential in the implementation of such ocean-wave sensors. Furthermore, the simple Bragg-scatter interpretation of the interaction process confirmed by the theory should permit the design of a variety of bistatic (Barrick [16], Peterson *et al.* [25]) as well as backscatter experiments for the monitoring of ocean waves.

For example, a ship equipped with a broad-band omnidirectional vertical monopole could serve as a backscatter radar.[3] The average scattered power from a circular range cell at a given radio wavenumber k_0 will be directly proportional to the ocean-wave height spectrum evaluated at spatial wavenumber $2k_0$. By sweeping frequency from about 1 to 20 MHz, the significant portion of the lower end of the gravity wave spectrum can be measured. Furthermore, directionality of ocean-wave movement can be ascertained because the ship's velocity imposes a unique Doppler bias on the first-order sea-scatter shifts versus bearing from the ship heading. Such a technique, employing the quantitative model set forth in this paper, could prove to be a useful tool for detailed oceanographic studies of directional wave height spectra.

REFERENCES

[1] D. D. Crombie, "Doppler spectrum of sea echo at 13.56 Mc/s," *Nature*, vol. 175, pp. 681–682, 1955.
[2] W. H. Peake, "Theory of radar return from terrain," in *1959 IRE Int. Conv. Rec.*, vol. 7, pt. 1, pp. 27–41.
[3] S. O. Rice, "Reflection of electromagnetic waves from slightly rough surfaces," in *Theory of Electromagnetic Waves*, M. Kline, Ed. New York: Interscience, pp. 351–378.
[4] D. E. Barrick and W. H. Peake, "A review of scattering from surfaces with different roughness scales," *Radio Sci.*, vol. 3, pp. 865–868, 1968.
[5] N. W. Guinard and J. C. Daley, "An experimental study of a sea clutter model," *Proc. IEEE*, vol. 58, pp. 543–550, Apr. 1970.
[6] J. W. Wright, "A new model for sea clutter," *IEEE Trans. Antennas Propagat.*, vol. AP-16, pp. 217–223, Mar. 1968.
[7] F. G. Bass, I. M. Fuks, A. I. Kalmykov, I. E. Ostrovsky, and A. D. Rosenberg, "Very high frequency radiowave scattering by a disturbed sea surface—parts I and II," *IEEE Trans. Antennas Propagat.*, vol. AP-16, pp. 554–568, Sept. 1968.
[8] P. Beckmann and A. Spizzichino, *The Scattering of Electromagnetic Waves from Rough Surfaces*. New York: Macmillan, 1963, p. 503.
[9] G. T. Ruck, D. E. Barrick, W. D. Stuart, and C. K. Krichbaum, *Radar Cross Section Handbook*, vol. 2. New York: Plenum, 1970, ch. 9.
[10] B. E. Parkins, "Coherence of acoustic signals reradiated from the time-varying surface of the ocean," *J. Acoust. Soc. Amer.*, vol. 45, pp. 119–123, 1969.
[11] J. R. Wait, "Electromagnetic surface waves," in *Advances in Radio Research*, vol. 1, J. A. Saxton, Ed. New York: Academic Press, 1964, pp. 157–217.
[12] G. D. Monteath, "Application of the compensation theorem to certain radiation and propagation problems," *Proc. Inst. Elec. Eng.*, vol. 98, pp. 23–30, 1951.
[13] R. J. King, "Electromagnetic wave propagation over a constant impedance plane," *Radio Sci.*, vol. 4, pp. 255–268, 1969.
[14] ——, "An introduction to electromagnetic surface wave propagation," *IEEE Trans. Educ.*, vol. E-11, pp. 59–61, Mar. 1968.
[15] D. E. Barrick and W. H. Peake, "Scattering from surfaces with different roughness scales: analysis and interpretation," Battelle Memorial Inst., Columbus, Ohio, Res. Rep. BAT-197-10-3, ASTIA Doc. AD662751; also ElectroScience Lab., Ohio State Univ., Columbus, Tech. Rep. 1388–26, N67–39091, 1967.
[16] D. E. Barrick, "The interaction of HF/VHF radio waves with the sea surface and its implications," in *AGARD Conf. Proc. Electromagnetics of the Sea* (no. 77), available from Clearinghouse for Federal Scientific and Technical Information, Springfield, Va., accession no. AD716305, 1970.
[17] O. M. Phillips, *Dynamics of the Upper Ocean*. London: Cambridge Univ. Press, 1966, pp. 109–139.
[18] W. H. Munk and W. A. Nierenberg, "High frequency radar sea return and the Phillips saturation constant," *Nature*, vol. 224, p. 1285, 1969.

[19] C. Cox and W. H. Munk, "Measurement of the roughness of the sea surface from photographs of the sun's glitter," *J. Opt. Soc. Amer.*, vol. 44, pp. 838–850, 1954.

[20] L. A. Berry and M. E. Chrisman, "A Fortran program for calculation of ground wave propagation over homogeneous spherical earth for dipole antennas," Nat. Bur. Stand., Boulder, Colo., Rep. 9178, 1966.

[21] D. E. Barrick, "Theory of HF/VHF propagation across the rough sea—parts I and II," *Radio Sci.*, vol. 6, pp. 517–533, 1971.

[22] J. M. Headrick, private communication, Nav. Res. Lab., Washington, D. C., 1970.

[23] D. D. Crombie, J. M. Watts, and W. M. Berry, "Spectral characteristics of HF ground wave signals backscattered from the sea," in *AGARD Conf. Proc. Electromagnetics of the Sea* (no. 77), available from Clearinghouse for Federal Scientific and Technical Information, Springfield, Va., Accession no. AD716305, 1970.

[24] J. F. Ward, "Power spectra from ocean movements measured remotely by ionospheric radio backscatter," *Nature*, vol. 223, pp. 1375–1330, 1969.

[25] A. M. Peterson, C. C. Teague, and G. L. Tyler, "Bistatic radar observation of long-period directional ocean-wave spectra with LORAN A," *Science*, vol. 170, pp. 158–161, 1970.

Temporal Frequency Spectra of Multifrequency Waves in Turbulent Atmosphere

AKIRA ISHIMARU, SENIOR MEMBER, IEEE

Abstract—General formulations for temporal frequency spectra of the fluctuations of plane, spherical, and beam waves operating at two frequencies are given based on weak turbulence and frozen-in assumptions. The cross spectra and the coherence are obtained for the amplitude at two frequencies, the phase at two frequencies, and the amplitude at one frequency and the phase at another frequency. The results are examined in detail for plane and spherical waves. For the spectrum of the index of refraction κ^{-n} in the inertial subrange, the amplitude spectrum behaves as $k^{(5-n)/2}$ for $\omega \to 0$ and $k^2\omega^{1-n}$ for $\omega \to \infty$. The phase spectrum for $\omega \to 0$ and for $\omega \to \infty$ behaves as $k^2\omega^{1-n}$ with different constants. These results agree well with the experimental work of Janes *et al.* [11] at 9.6 and 34.5 GHz, and explains the ratio of the spectra at two frequencies. Also noted is the experimental slope of -2.6 as $\omega \to \infty$ which may be compared with $1 - n = -2.66$ using the Kolmogorov spectrum of $n = 11/3$. The amplitude and phase coherence are calculated, and the results agree well with the experimental data. This agreement is indicative of the general validity of the theory for frequencies as low as 10~30 GHz and the path length as long as 60 km. It is also shown that using the preceding theory, the wind velocity and the structure constant C_n can be deduced from the experimental data. Theoretical wind velocity of 15.6 knots obtained from the propagation data compares favorably with the meteorologically measured value of 14 knots, and two values of C_n obtained independently from the amplitude and phase measurements closely agree with each other.

I. Introduction

THE FLUCTUATIONS of a wave propagating in turbulent atmosphere have been extensively studied in the past [1]–[5], and the temporal frequency spectrum of the amplitude fluctuations of a plane wave have been

given by Tatarski [1]. Lawrence and Strohbehn have discussed more recent work by Tatarski on temporal spectra of amplitude and phase fluctuations [6]. Mandics and Lee [7] also discussed the correlations of a wave observed at two frequencies.

However, recent interest in remote probing of turbulent atmosphere created the need for more complete theoretical treatment of the wave propagation in atmosphere. Specifically, at millimeter and optical wavelength, there is a need to extend the previous work on a beam wave [3], [4] to include the temporal frequency spectra and multifrequency observations.

This paper presents general formulations for temporal frequency spectra of the fluctuations of waves operating at two frequencies. The results are examined in detail for plane and spherical waves and compared with the experimental work of Janes *et al.* [11] at 9.6 and 34.5 GHz. The general agreement with the experimental data indicates the general validity of the theory. It is also shown how the propagation data may be used to infer the wind velocity and C_n.

II. General Formulations of Problem

We consider a turbulent medium characterized by the index of refraction

$$n(\bar{r},t) = 1 + n_1(\bar{r},t) \tag{1}$$

where $n_1(\bar{r},t)$ is the fluctuation and assumed to be small. Assuming the frozen-in hypothesis, we have

$$n_1(\bar{r},t) = n_1(\bar{r} - \bar{V}t, 0) \tag{2}$$

where $\bar{V}$ is the average wind velocity vector. This assumption represented by (2) means that the effect of the velocity fluctuations is small compared with the average wind